IEEE Access
Multidisciplinary | Rapid Review | Open Access Journal

Received March 20, 2022, accepted April 6, 2022, date of publication April 14, 2022, date of current version April 20, 2022.

Digital Object Identifier 10.1109/ACCESS.2022.3167395

Optimal Planning of Multiple Renewable Energy-Integrated Distribution System With Uncertainties Using Artificial Hummingbird Algorithm

MD. SHADMAN ABID, (Student Member, IEEE), HASAN JAMIL APON, KHANDAKER ADIL MORSHED, AND ASHIK AHMED

Department of Electrical and Electronic Engineering, Islamic University of Technology, Gazipur 1704, Bangladesh

Corresponding author: Md. Shadman Abid (shadmanabid@iut-dhaka.edu)

ABSTRACT Appropriate installation of renewable energy-based distributed generation units (RDGs) is one of the most important challenges and current topics of interest in the optimal functioning of modern power networks. Due to the intermittent nature of renewable energy sources, optimal allocation and sizing of RDGs, particularly photovoltaic (PV) and wind turbine (WT), remains a critical task. Based on a new metaheuristic known as the Artificial hummingbird algorithm (AHA), this paper provides a novel approach for addressing the problem of RDG planning optimization. Considering various operational constraints, the optimization problem is developed with multiple objectives including power loss reduction, voltage stability margin (VSM) enhancement, voltage deviation minimization, and yearly economic savings. Furthermore, using relevant probability distribution functions, the ambiguities related with the stochastic nature of PV and WT output powers are evaluated. The proposed algorithm was compared to two of the recent metaheuristics applied in this domain known as improved harris hawks and particle swarm optimization algorithm (HHO-PSO) and hybrid of phasor particle swarm and gravitational search algorithm (PPSOGSA). The IEEE 33-bus and 69-bus systems are assessed as the test systems in this study. According to the findings, AHA delivers superior solutions and enhances the techno-economic benefits of distribution systems in all the scenarios evaluated.

INDEX TERMS Distributed generation, optimal DG placement, artificial hummingbird algorithm, renewable energy, voltage stability margin, voltage stability, distribution system planning, wind turbine, photovoltaic generation.

NOMENCLATURE

b	Branches index.
i	Bus index.
m	RDG index.
N_{BR}	The total number of branches in the system.
N_B	The total number of buses in the system.
N_{DG}	The total number of RDGs in the system.
$N_{iter,max}$	Maximum number of iterations.
N_{pop}	Population size.
N_{runs}	Total individual runs.
v_{co}	Cut-out wind speed of WT.
μ	Total DG penetration level.
C, K	Scale and shape parameters of Weibull function.
α, β	Scale and shape parameters of Beta function.
C_{DG}	Cost per kW of injected RDG power .
G_{stc}	the solar irradiance at standard test conditions.
R_c	Certain irradiance point.
$S_{DG,max}$	Allowable maximum size of single RDG.
$S_{DG,m}$	Size of m^{th} DG.
T_{DG}	Total DG lifetime in years.
V_i^{ref}	Magnitude of the reference voltage at i^{th} bus.
v_{ci}	Cut-in wind speed of WT.
V_{i-max}	Maximum allowable voltage value of i^{th} bus.
V_{i-min}	Minimum allowable voltage value of i^{th} bus.
v_n	Nominal wind speed of the wind turbine.
C_E	Average cost of energy loss per kWh.
P_{PVR}	Rated output power of PV unit.
P_{WTR}	Rated output power of WT unit.
R	Rate of interest on capital investment of the installed DG.

The associate editor coordinating the review of this manuscript and approving it for publication was Ehab Elsayed Elattar.

Γ	Gamma function.
μ^t	Mean deviation at the t time interval.
σ_t	Standard deviation at the t time interval.
$AEL_{T,DG}$	Total annual economic loss with RDG.
$AEL_{T,noDG}$	Total annual economic loss without DG.
CRF	Capital recovery factor.
G	Solar irradiance on the PV module surface.
$Iter$	Current iteration.
$P_{DG,m}$	Active power output of m^{th} DG.
$P_{loss,b}$, $Q_{loss,b}$	Active and reactive power loss of bus b.
$P_{loss,no-DG}$	Total active power loss without integrating RDGs.
$P_{loss,RDG}$	Total active power loss after integrating RDGs.
P_{loss}	Total active power loss.
P_{PVg}	Power generation of the photovoltaic unit.
P_{slack}, Q_{slack}	Active and reactive power injected by the slack bus.
P_{WTg}	Power generation of the wind turbine.
pf_{PV}	Power factor of PV unit.
pf_{WT}	Power factor of WT unit.
r	Random number uniformly distributed on [0, 1].
$rand$	random number between [0,1].
$TAES$	Total annual energy saving.
v	Wind speed at the hub height of the WT.
V_i	Voltage magnitude at bus i.
f_s	Beta PDF of solar irradiance.
f_v	Weibull PDF of wind speed.

I. INTRODUCTION

The demand for electricity is increasing all around the world due to advancements in science and technology. The existence of industrial activities and social structures relies mostly on low cost and uninterrupted supply of electrical energy [1]. Although fossil fuels are the primary source of power generation, their resources are rapidly depleting, putting the future of fossil fuels in jeopardy. As a result, the current tendency is to use renewable energy sources such as solar energy, wind energy, water energy, and nuclear energy to generate electricity. Optimal integration and planning of RDG unit installation (such as WTs and PVs) in distribution networks can be a feasible solution to the difficulties associated with conventional energy source scarcity.

Various studies have been conducted over the years investigating the potential benefits, challenges and scopes of RDG implementation on distribution networks. For instance, the authors of [2] highlight the major concerns, possibilities, and constraints of integrating distributed generation into electric power networks. Renewable energy sources are now the most convenient and profitable source of DGs. Moreover, [3] depicts the future prospects and scientific developments to harness renewable energy sources. Various sources of renewable energy and their benefits, growth, investment and deployment have been illustrated. Along with these works, many of the studies like [4]–[7] have explored the integration of renewable energy sources into electric power systems and smart power grids, taking into account the availability of renewable energy sources. RDGs are gaining attraction as a solution for high power demand to reduce dependency on diminishing coal, fossil fuels, and natural gas. For instance, the authors of [8] suggest a comprehensive review of grid-integrated DG planning. Additionally, depending on certain factors such as generator type, penetration level, and grid features, the influence of RDGs on the distribution grid has been demonstrated in [9]. It should be noted that electricity generated from renewable energy sources is heavily influenced by external factors such as temperature, weather, wind speed, and humidity. The work in [10] discusses the financial issues as well as the broader economic and societal effects of distributed energy generation. Besides, the authors of [11] explore the environmental advantages of dispersed energy resources and their influence on lowering greenhouse gas emissions. The authors of [12] established RDG planning and scheduling approach using uncertainty modeling methodologies to provide techno-economic and environmental benefits. Furthermore, [13] creates an efficient operational schedule for multi-grid distribution systems while taking into account the uncertain environment of energy storage systems. Moreover, the works in [14] present a planning framework to increase the resilience of power-water distribution networks, with the goal of lowering the investment costs associated with the suggested techniques. In order to optimize techno-economic benefits, the authors of [15] utilize an algorithm for optimum integration of DGs in active distribution system (ADS) networks.

The energy provided by RDG sources is heavily influenced by factors like weather, temperature, site location, and time. The primary research problem in this subject is to deal with uncertainty in DG integrated power system networks. Furthermore, unregulated and inappropriate RDG unit penetration in distribution networks may impair system performance. Several studies have been conducted in the field of optimal sizing and allocation or placement of multiple and multi-type DGs in distribution systems employing optimization techniques. For instance, [16] discusses some approaches which can handle uncertainties like monte carlo simulation (MCS), scenario-based analysis (SBA), point estimate method (PEM) etc. A monte carlo simulation (MCS) based probabilistic method has been designed in [17] to examine the impact of wind power and PV power generation on distribution networks. Besides, [18] takes the help of MCS and particle swarm optimization (PSO) for optimal sizing of renewable energy systems considering stochastic behaviour of energy resources. The authors in [19] proposed improved harris hawks based particle swarm optimizer (HHO-PSO) for integrating renewable energy sources into distribution networks incorporating PV and WT generation uncertainties. Furthermore, [20] suggests a hybrid mix of phasor particle swarm optimization and gravitational search algorithm (PPSOGSA) for integrating

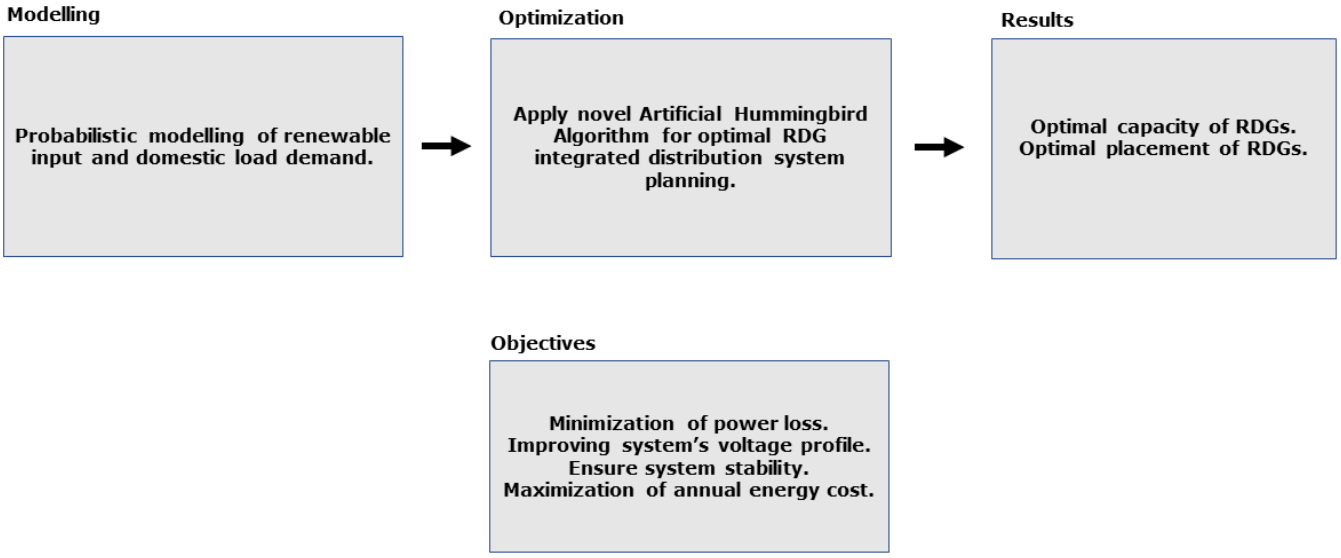

FIGURE 1. Steps of current research work.

renewable energy sources into distribution networks while accounting for PV and WT generation and load uncertainties. In [21], an optimization technique called ant lion optimization algorithm (ALOA) has been introduced for optimal sizing and allocation of RDGs in a radial distribution network. Besides, in many of the works [22]–[28], backtrack search optimization algorithm (BSOA), artificial bee colony (ABC) algorithm, hybrid grey wolf optimizer, bacterial foraging optimization algorithm (BFOA), intelligent water drop (IWD) algorithm, stud krill herd algorithm (SKHA), and combined genetic algorithm-particle swarm optimization (GA-PSO) algorithm techniques were proposed for optimal DG sizing and placement. Moreover, optimization methods like mixed-integer non-linear programming (MINLP), multi-objective opposition based chaotic differential evolution (MOCDE) and evolutionary programming (EP) based technique have been suggested for optimal placement and sizing of DGs aiming loss minimization, and other techno-economic benefits [29]–[31]. The research in [32] employs the diagonal band Copula and the sequential monte carlo approach to optimally locate stochastic RDGs in imbalanced distribution power networks. Besides, [33] proposes a weighted aggregation PSO approach for tackling the selection of solar and wind RDGs based on their stochastic nature. Furthermore, the authors presented a bi-level metaheuristic method in [34] to solve the complex modelling approach of renewable energy sources and EV management in order to accomplish autonomous microgrids. In addition, [35] proposes an optimization technique for determining the ideal placements and sizes of solar and wind generation systems while also managing EVs to assemble an autonomous microgrid. [36] presents quasi-reflection based slime mould algorithm (QRSMA) for solving optimal allocation and sizing problems of capacitors and distribution generations. Moreover, the authors in [37] have discussed optimal allocation of renewable distributed generation (RDG) into distribution systems considering seasonal uncertainties of solar-wind load demands. [38] proposes a new approach for optimal scheduling of renewable-based multi-energy microgrid (MEM) systems which focuses on robust optimization with flexible energy conversion and storage devices. A multi-objective probabilistic approach has been adopted in [39] for smart voltage control of wind-energy integrated systems. Furthermore, [40] presents comprehensive research on multi-objective optimization of multiple energy integrated stations for improving energy conversion and utilization efficiency.

The RDG planning research domain also includes realistic distribution networks that use real-time data. For instances, in the works of [41], the whale optimization technique (WOA) algorithm was evaluated on IEEE 15-bus, 33-bus, 69-bus, and actual distribution networks like 85-bus and 118-bus test systems to determine the optimal DG-units size. Furthermore, the authors of [42] introduced a robust and effective technique called hybrid particle swarm optimization combined with gravitational search algorithm (PSOGSA) and MMFO for determining the optimal location and capacity of RDG units for minimizing system power losses and operating costs while improving voltage profile and voltage stability. For simulation purposes, MEDN 15-bus and Moscow 111-bus practical test scenarios were analyzed. Besides, the authors of [43] proposed the power voltage sensitivity constant (PVSC) as a solution to the RDG allocation problem. A new metric is also proposed, which takes into account the amount of DG penetration as well as the percentage decrease in real power losses. The suggested technique's findings have been validated on a conventional IEEE 33 bus system and a 130 bus actual distribution system in Jamawaramgarh, Jaipur. Additionally, the indicators of loss sensitivity factors and bus voltage magnitudes are included in [44] to construct a set of fuzzy expert rules for asserting the preliminary buses for distributed generator placement. The suggested backtracking search technique (BSA) approach enables the fuzzy decision-maker to select the best option among the pareto-optimal choices available. On 33- and 94-node radial distribution networks with varied situations, the key aspects

of the BSA technique are evaluated. Moreover, in the works of [45], the efficacy of an appropriate control mechanism is demonstrated with case studies for deterministic RDG placement on base configurations of IEEE 30-bus and 57-bus systems utilizing the SHADE-EC algorithm. The SHADE-EC method is also used to solve the single-objective and multi-objective stochastic instances.

A. PROBLEM STATEMENT

Uncontrolled and excessive RDG unit penetration in distribution networks can have a negative impact on system performance. The prospect of bidirectional power flow, as well as difficulties such as higher power losses, voltage drop, reactive power management, and power quality issues, are among these concerns. Therefore, integration of RDG units in distribution networks necessitates much attention and proper planning to ensure the performance of the electrical network, such as system reliability, power quality, total active power loss reduction, and economic efficiency can be met. Besides, the power generated from RDG sources is mostly dependent on uncertainties like weather, temperature, location of site and time. The key challenge is to cope with uncertainties in DG integrated power system networks. Several studies have been conducted in the field of optimal sizing and allocation or placement of multiple and multi-type DGs in distribution systems employing different optimization techniques. The majority of these works are aimed at improving the distribution network's technical parameters in terms of power loss reduction and voltage stability. Besides, the preceding studies indicate that determining the appropriate RDG location for distribution networks is a continuous challenge. The significance of optimization techniques in this research domain cannot be overestimated, as it would be advantageous if major improvements could be achieved utilizing a novel or modified optimization technique.

B. RESEARCH GAPS

Based on the aforementioned literature review, the following findings may be formed:

- Very limited works have been published on optimal RDG allocation and size when PV and WT generation uncertainties are combined with load uncertainties.
- The majority of previous studies have ignored the techno-economic assessment of the proposed techniques.
- The voltage stability margin index (VSM_{sys}) has yet to be investigated in this research domain.
- AHA is unexplored in the research domain of RDG sizing and allocation when load and generation uncertainties are considered.

C. MAIN CONTRIBUTION

The objective of this research is to evaluate the location and sizing of RDGs in order to minimize active power loss, maximize system voltage stability margins, minimize voltage deviation, and maximize overall yearly energy savings costs. The following is a list of the current work's major contributions:

- PV and WT power generation, as well as load variation, are all factored into the RDG sizing and allocation problem.
- The stochastic characteristics are achieved by using appropriate probability density functions (PDFs).
- The Artificial hummingbird algorithm (AHA), a recently developed algorithm, is used to determine the optimal solution with high exploitation potential and exploration aptitude.
- The performance of the suggested AHA is assessed, and its superiority over two of the most recent metaheuristics used in this domain known as hybrid phasor particle swarm optimization and gravitational search algorithm (PPSOGSA) [20] and improved harris hawks based particle swarm optimizer (HHO-PSO) [19] is demonstrated.
- Several scenarios of PV and WT penetration are explored to test the algorithm's efficacy, including and excluding uncertainties.
- In all the scenarios evaluated, AHA provides superior solutions and improves the techno-economic aspects of distribution networks.

The rest of the paper is organized as follows: Section II outlines the modelling approach, Section III presents AHA, Section IV describes the problem formulation, Section V presents the solution procedure, Section VI illustrates the simulation results, and Section VII concludes this work.

II. MODELLING

Renewable power is primarily affected by weather conditions such as solar irradiation, temperature, wind speed, etc. As a result, before planning the integration of RDG units into electrical networks, the uncertainties and unpredictable behaviour of renewable output power should be assessed extensively. Monte carlo simulation method is a probabilistic approach is the most used method to characterize power system uncertainties [16]. Besides, weibull and beta functions were used to model the uncertainty of wind speed and solar irradiance, respectively [18], [20]. For the purpose of this study, historical weather information for one year has been collected to obtain a typical annual profile for stochastic behaviour pattern of solar irradiance and wind speed [24], [46].

A. MODELLING OF WT

A wind turbine's power generated, P_{WT}, can be formulated as [33], [47] :

$$P_{WT}(v) = \begin{cases} 0, & for\ v \le v_{ci} \\ \dfrac{v - v_{ci}}{v_n - v_{ci}} * P_{WTR}, & for\ v_{ci} < v \le v_n \\ P_{WTR}, & for\ v_n < v \le v_{co} \\ 0, & for\ v \ge v_{co} \end{cases} \quad (1)$$

The stochastic nature of wind resources in a specific location can be evaluated by utilizing the following weibull probability density function:

$$f_v(v) = K/C * (v/C)^{K-1} * e^{-(v/C)^K} \quad (2)$$

The weibull function's cumulative distribution function can be expressed as Eq.(3) while wind speed can be

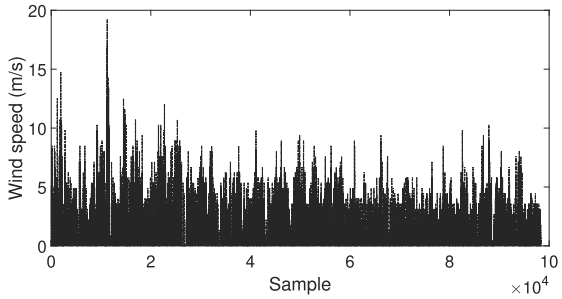

FIGURE 2. Wind speed test data [46].

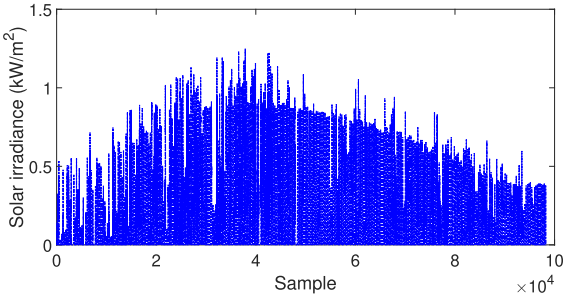

FIGURE 3. Solar irradiance test data [46].

determined from its inverse as shown in Eq.(4).

$$F_v(v) = 1 - e^{-(v/C)^K} \tag{3}$$

$$v = C * [-ln(r)]^{(1/K)} \tag{4}$$

where, k and C are the shape factors whose expected values can be found using the average and standard deviation (std) of the wind speed measurements in a period t can be expressed as Eq.(5) and Eq.(6).

$$K^t = (\sigma_v^t/\mu_v^t)^{-1.086} \tag{5}$$

$$C^t = \mu_v^t/\Gamma(1 + 1/K^t) \tag{6}$$

Weibull PDF can be expressed in discrete form by sub-dividing the considered time interval t into N_v states. By considering g as the inverse of N_v, Eq.(2) and Eq.(5) can be re-written and the forecasted WT power can be formulated as Eq.(7).

$$P_{WT} = [\sum_{g=1}^{N_v} P_{WTg} * f_v(v_g^t)]/[\sum_{g=1}^{N_v} f_v(v_g^t)] \tag{7}$$

where, $v = v_g^t$ and $f_v\ (v_g^t)$ refers to the probability of wind speed at t^{th} time interval for the g^{th} state.

B. MODELLING OF PV

Power generated from PV units significantly depends on solar irradiance and it can be formulated as [33], [47]:

$$P_{PV}\ (G) = \begin{cases} (P_{PVR} * G^2)/(G_{STC} * R), & for\ G < R_c \\ (P_{PVR} * G)/G_{STC}, & for\ G > R_c \end{cases} \tag{8}$$

The beta probability density function is used to achieve realistic PV unit modelling by considering the stochastic behaviour of solar irradiation.

$$f_s\ (G) = \begin{cases} [\Gamma(\alpha + \beta)/(\Gamma(\alpha) * \Gamma(\beta))] * G^{(\alpha+1)} * (1 - G)^{(\beta-1)} \\ \quad for\ 0 \le G \le 1, \alpha \ge 0, \beta \ge 0 \\ 0, \quad otherwise \end{cases} \tag{9}$$

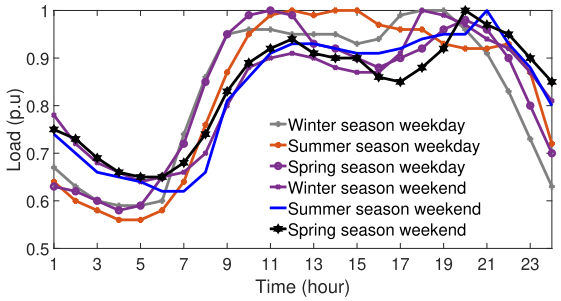

FIGURE 4. IEEE reliability test system (RTS) load data [48].

where α and β are the shape factors of beta function which can be determined by considering the average and standard deviation of the solar irradiance as shown in Eq.(10) and Eq.(22).

$$\beta^t = (1 - \mu_G^t) * [(\mu_G^t * (1 + \mu_G^t)/(\sigma_G^t)^2) - 1] \tag{10}$$

$$\alpha^t = (\mu_G^t * \beta^t)/(1 - \mu_G^t) \tag{11}$$

Beta PDF can be taken into discrete form by sub-dividing the considered time interval t into N_s states. Thus, re-writing the Eq.(9) while considering g from 1 to N_s, the forecasted PV generated power can be formulated as Eq.(12).

$$P_{PV} = [\sum_{g=1}^{N_s} P_{PVg} * f_s(S_g^t)]/[\sum_{g=1}^{N_s} f_s(S_g^t)] \tag{12}$$

where, $f_s(G_g^t)$ refers the solar irradiance probability at t^{th} time interval for g^{th} state.

C. LOAD MODELLING

The normal probability distribution function can be used to define load patterns for each hour of a specified daily load [20].

$$f_L(L) = \frac{1}{\sqrt{2\pi}\sigma_L} e^{-\frac{(L-\mu_L)^2}{2\sigma_L^2}} \tag{13}$$

$$f_L(L) = (1/2)\ (1 + erf((L - \mu_L)/\sqrt{2}\sigma_L) \tag{14}$$

$$L = \mu_L + \sqrt{2}\sigma_L * erf^{-1}(2r - 1) \tag{15}$$

where L is a random variable that represents load, and μ_L, σ_L represent the average and std of L, correspondingly. $erf\,(.)$ and $erf^{-1}(.)$ signify the error and inverse error functions, respectively, and r is a random number between 0 and 1.

Hour, t is divided into N_L states for convenience, and the associated load and probability value for each state can be determined using Eqs.(14) and (15), accordingly. L can be reformulated as :

$$L^t = \sum_{g=1}^{N_L} L_g f_L(L_g^t) / \sum_{g=1}^{N_L} f_L(L_g^t) \tag{16}$$

where L_g^t refers the load of state g at hour t; L_g is the load level at state g and $f_L(L_g^t)$ is the probability of the load level of the state g at hour t. The load data for different seasons are collected from [48].

III. ARTIFICIAL HUMMINGBIRD ALGORITHM

A hummingbird explores aspects such as the nectar amount and quality of certain flowers, as well as the nectar-refilling mechanism in order to pick a suitable source from a variety of

food sources. Hummingbirds' unique flying skills and precise foraging methods for accessing food sources inspired this algorithm, which varies from prior algorithms in terms of search domain diversity. The different flying patterns ensure that the algorithm has a high exploitation probability and exploration ability. Besides, a unique component called the visit table is also included in order to simulate the hummingbird's memory for identifying suitable food sources. Hummingbirds employ three foraging approaches and three flying skills to collect food from sources [49]. The three different flying patterns are known as axial, diagonal, and omnidirectional, as well as the three different search strategies are known as guided foraging, territorial foraging, and migration foraging. The following section includes three mathematical models that simulate three hummingbird foraging habits.

A. INITIALIZATION

A swarm of n hummingbirds is arbitrarily assigned to n food sources, as follows:

$$x_w = LB + rand(UB - LB) \quad w = 1 \ldots, n \tag{17}$$

where LB and UB, respectively represent the upper and lower bounds of a d-dimensional problem. $rand$ is a random vector in the range [0, 1] and the location of the w^{th} food supply that provides the solution to the particular objective is represented by x_w. The visit table of the source of food can be specified as:

$$VT_{w,e} = \begin{cases} 0, & \text{if } w \neq e \quad w = 1 \ldots, n \\ null, & \text{if } w = e \quad e = 1 \ldots, n \end{cases} \tag{18}$$

when $w = e$, the value of $VT_{w,e}$ becomes null which means that a hummingbird is collecting its food from its particular source. Moreover, when $w \neq e$ the value of $VT_{w,e}$ becomes zero which implies that the e^{th} food source has been very recently searched by the w^{th} hummingbird in the current iteration.

B. GUIDED FORAGING

Every hummingbird has a general tendency for foraging the source of food with the most nectar volume, which implies that an intended source must possess a high replenishing rate of nectar and a lengthy interval without any visit. Three flying methods: omnidirectional, diagonal, and axial flights are utilized by providing a direction switch vector during foraging. This vector is utilized to determine if one or more d-dimension space directions are accessible. Most birds can fly omnidirectionally, but hummingbirds can also glide axially and diagonally. The axial flight can be expressed as:

$$D^{(w)} = \begin{cases} 1, & \text{if } w = randi([1, d]) \quad w = 1, \ldots, d \\ 0, & \text{else} \end{cases} \tag{19}$$

The diagonal flight can be expressed as:

$$D^{(w)} = \begin{cases} 1, & \text{if } w = Pp(j), j \in [1, k] \\ & Pp = randperm(Kp) \\ & Kp \in [2, [r_1 \cdot (d-2)] + 1] \\ 0, & \text{else } w = 1, \ldots, d \end{cases} \tag{20}$$

TABLE 1. Artificial hummingbird algorithm pseudo code.

```
Algorithm : Pseudo-code of AHA
Define N_pop = n = Population size
Define N_iter,max
Define higher and lower bound of the population
Initialize the population using eq. (17)
while tp ≤ N_iter,max
    for Each population calculate direction switch vector D
    if rand ≤ 1/3
    Follow diagonal flight using eq. (20)
    else if rand≤ 2/3
     Follow omnidirectional flight using eq. (21)
    else Follow axial flight using eq. (19)
    end if
    end for
            for Each population update foraging behaviour
            if rand ≤ 0.5
            Follow guided foraging using eqs. (19) to (24)
            else if Follow territorial foraging eqs. (25) and (26)
            end if
            if  tp = 2n
            Follow migration foraging using eq. (27)
            end if
            end for
Update positions
Return the best fitness value
tp= tp+1
end while
```

The omnidirectional flight can be expressed as :

$$D^w = 1 \quad i = 1, \ldots., d \tag{21}$$

where, an arbitrary integer between 1 and d is returned by $randi$. An arbitrary permutation sequence of integers between 1 and Kp is generated by $randperm(Kp)$. r_1 is a random value between 0 and 1. Therefore, a food source is upgraded in terms of the target food source, which is identified from the current sources. Hence, the equation to replicate directed foraging is as follows:

$$vp_w = x_{w,tar}(tp) + a.D.(x_w(tp) - x_{w,tar}(tp)) \tag{22}$$

$$a \sim N(0, 1) \tag{23}$$

$x_w(tp)$ defines the location of the w^{th} source of food at current iteration tp, $x_{w,tar}(tp)$ is the location of the source of food that the w^{th} hummingbird plans to consume from, and that denotes a normal distribution with a mean value of zero and a standard deviation of one. Moreover, Eq.(22) allows each present source to modify its location with relation to the intended source of food and replicates guided foraging in hummingbirds using various flying patterns. Hence, the location of the w^{th} food source is updated as follows:

$$x_w(tp+1) = \begin{cases} x_w(tp), & \text{if } f(x_w(tp)) \leq f(vp_w(tp+1)) \\ v_w(tp+1), & \text{if } f(x_w(tp)) > f(vp_w(tp+1)) \end{cases} \tag{24}$$

where f signifies the fitness value of the function. According to Eq.(24), if the candidate food source's nectar-refilling rate is greater than the present one, the hummingbird leaves the present source of food and consumes from the candidate food source following Eq.(22). The visit table is a key component of the AHA algorithm that retains the information about the visit to the sources of food. The visit table records how long each food source has been undiscovered, and a long

undiscovered period indicates a high degree of visit. Through Eq.(22), every bird of the swarm accesses its desired source of food. When a bird undergoes guided foraging utilizing Eq.(22), keeping in mind of its targeted source of food during each iteration, the visit levels of all the other sources are increased by one.

C. TERRITORIAL FORAGING

When the nectar of the flower has been exhausted, a hummingbird prefers to seek out a new source of food than it is to visit other current food sources. As a result, a hummingbird might easily migrate to an adjacent location within its own region, where a new food supply may be discovered. The mathematical equation for modelling hummingbirds' territorial foraging behaviour is as follows:

$$vp_w(tp+1) = x_w(tp) + bp.D.x_w(tp) \tag{25}$$

$$bp \sim N(0,1) \tag{26}$$

The territorial factor, bp, has a mean value of zero and a standard deviation of one and follows a normal distribution. By using its specific flight talents as Eq. 25, every hummingbird can swiftly identify a new source of food in its nearby surroundings.

D. MIGRATION FORAGING

If the number of iterations surpasses the previously specified migration coefficient value, the bird which is at the source of food with the lowest replenishing rate of nectar will arbitrarily look for a new source of food within the territory. A hummingbird's migratory foraging to a destination might be described as follows:

$$x_{wor}(tp+1) = LB + rand(UB - LB) \tag{27}$$

Here, x_{wor} is the source of food with the lowest replenishing rate of nectar. The following is a preferred definition for the migration coefficient in terms of population size (n):

$$tp = 2n \tag{28}$$

According to Eq. (22), in the initial stages of iterations, exploration is stressed due to the significant distance between food sources, but as the number of iterations increases, the distance iteratively reduces, and therefore exploitation is prioritized.

IV. PROBLEM FORMULATION

Incorporating RDGs complicates the optimal placement problem due to having unpredictable and stochastic properties [45]. Therefore, non-linear, constrained and discrete optimization should be incorporated in the planning methods.

A. OBJECTIVE FUNCTION

The fundamental objective of this work is to maximize the techno-economic benefits of RDGs in distribution networks. Several aspects are explored to comprehend the simulation, including active power loss minimization, bus voltage improvement, network voltage stability margin (VSM) enhancement, and yearly economic loss reduction. Using the weighted sum approach, these four evaluation criteria can be integrated into a single objective function.

$$OF = min\ (\omega_1 * OF_1 + \omega_2 * OF_2 + \omega_3 * OF_3 + \omega_4 * OF_4) \tag{29}$$

where, OF_1, OF_2, OF_3, OF_4 denotes the reduction in total active power losses, strengthening bus voltages by minimizing voltage deviation, improvement of VSM of the network, increasing the amount of total annual energy saving, respectively. ω_1, ω_2, ω_3, ω_4 represents the weighted factors assigned to OF_1, OF_2, OF_3, OF_4 respectively and total sum of absolute values of ω_1, ω_2, ω_3, ω_4 is considered to be equal to 1. It should be noted that all weighted factors are considered to be the same with a value of 0.25. Furthermore, all the values of Eq.(29) are in per unit (p.u.) values. The four components of OF can be expressed mathematically like following equations.

$$OF_1 = P_{loss} = \sum_{b=1}^{N_{BR}} P_{loss,b} \tag{30}$$

$$OF_2 = V_D = \sum_{i=1}^{N_B} |V_i - V_i^{ref}| \tag{31}$$

V_D is considered as the total voltage deviation while V_i denotes the actual voltage magnitude (p.u) at i^{th} bus and V_i^{ref} represents 1.0 (p.u) of voltage magnitude.

$$OF_3 = \frac{1}{VSM_{sys}} \tag{32}$$

$$OF_4 = \frac{1}{TAES} \tag{33}$$

where,

$$TAES = AEL_{T,no\ DG} - AEL_{T,DG} \tag{34}$$

$$AEL_{T,noDG} = P_{loss,no-DG} * C_E * 8760 \tag{35}$$

$$AEL_{T,DG} = P_{loss,RDG} * C_E * 8760 + [(C_{DG} * \sum_{m=1}^{N_{DG}} P_{DG,m})/CRF] \tag{36}$$

$$CRF = [R * (1+R)^{T_{DG}}]/[(1+R)^{T_{DG}} - 1] \tag{37}$$

B. CONTROL VARIABLES

Positions, or indices of connected buses, and the number of elementary RDG units that should be connected at these buses are the control variables in this optimization problem. Considering these two variables, the RDG farms' optimum rated power can be determined as:

$$P_{RDGF} = N_{RDG} * P_{RDG} \tag{38}$$

where P_{RDGF} is the RDG farms' total rated power, N_{RDG} is the number of elementary RDG units that make up an RDG farm (WT farm or PV farm), and P_{RDG} is the rated power of an elementary RDG unit.

C. EQUALITY AND INEQUALITY CONSTRAINTS

To solve the provided objective function, a number of equality and inequality constraints are considered.

i. **Power balance equation** : The total real and reactive power provided from the grid (slack bus) and supplied by the RDGs should be equal to the real and reactive power demand of the loads, including real and reactive power losses.

$$P_{slack} + \sum_{m=1}^{N_{DG}} P_{DG,m} = \sum_{i=1}^{N_B} P_{D,i} + \sum_{b=1}^{N_{BR}} P_{Loss,b} \quad (39)$$

$$Q_{slack} + \sum_{m=1}^{N_{DG}} Q_{DG,m} = \sum_{i=1}^{N_B} Q_{D,i} + \sum_{b=1}^{N_{BR}} Q_{Loss,b} \quad (40)$$

ii. **Voltage limit** : Voltage magnitudes at each bus must be kept within certain limits.

$$V_{i-min} \leq V_i \leq V_{i-max} \quad (41)$$

iii. **Power flow limit** : The thermal limit of branch l should not be exceeded by the apparent power carried by it.

$$S_l \leq S_{l-max} \quad (42)$$

Total RDG generation must have maximum value, which is associated with the total load demand and a coefficient factor termed as μ. The coefficient μ is normally set in the range of (0.4-1) to avoid reverse power flow into the main substation [49]. In addition, the RDG power factor must stay within permissible limits.

$$\sum_{m=1}^{N_{DG}} S_{DG,m} = \mu \times \sum_{i=1}^{N_B} S_{D,i} \quad (43)$$

$$S_{DG,m} \leq S_{DG,max} \quad (44)$$

iv. **RDG Capacity Constraints** The active power capacity of each RDG farm is limited to a specific maximum.

$$N_{RDGi} * P_{RDGi} \leq NRDGi_{max} * P_{RDGi} \quad (45)$$

where N_{RDGi} is the number of elementary RDG units which comprises the RDG farm at location i; P_{RDGi} is the rated power of elementary RDG unit at location i; and $NRDGi_{max}$ is the maximum number of elementary RDG units at location i.

v. **VSM limit:** For efficient operation, the VSM_{sys} value of a distribution system should remain between 0.67 and 1.0 [51].

$$0.67 \leq VSM_{sys} \leq 1.0 \quad (46)$$

D. VOLTAGE STABILITY MARGIN

Voltage stability margin (VSM) [51] correlates voltage collapse and branch loading of a distribution network. Fig. 5 represents a radial feeder with a number of k branches whose loading indices, L_k can be formulated as:

$$L_k = (2\frac{V_v}{V_q} cos\delta_{qv} - 1)^2 \quad (47)$$

The voltage magnitudes of bus q and bus v are represented by V_q and V_v, respectively, whereas δ_{qv} specifies the phase angle difference between these buses. Now, VSM can be calculated as the product of all loading indices for all branches of the given radial feeder.

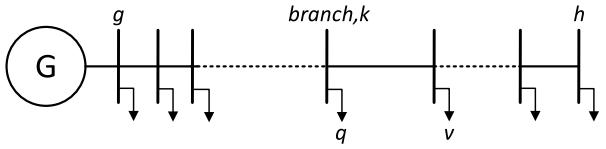

FIGURE 5. Radial feeder.

$$VSM = \prod_{l=\Omega} L_k \quad (48)$$

where Ω covers up all the branches of the radial feeder from the starting bus g to the ending bus h. If there are several feeders in a system, then VSM_{sys} is calculated as the VSM of the feeder with the minimum value.

$$VSM_{sys} = min(VSM_1, VSM_2, VSM_3, \ldots; VSM_{ssf}) \quad (49)$$

where ssf represents the system's total number of feeders.

E. TEST SYSTEMS DESCRIPTION

IEEE 33 bus [52] and IEEE 69 bus [53] distribution systems are employed as test systems in this work.

The one-line schematics for the IEEE 33 and IEEE 69 buses are shown in Fig. 6 and Fig. 7, respectively. The total load demand of the IEEE 33 bus system is 3.715 MW and 2.3 MVAr, whereas the total load demand of the IEEE 69 bus system is 3.802 MW and 2.695 MVAr. Furthermore, under normal operating conditions, total active power loss is 202.5 kW for the 33 bus system and 220.3 kW for the 69 bus system.

V. SOLUTION PROCEDURE

The following is a generic technique for using the proposed optimization algorithm to address the problem of optimal sizing and placement of RDG units in distribution networks.

Step 1: Set the network setup, bus data, branch specifications and load data.

Step 2: Specify the technical and economic information about the elementary RDG devices.

Step 3: Set the number of RDG farms (N_{RDGF}) that will be coupled to the network, as well as the maximum number and types of elementary RDG units that will be attached at a particular network bus.

Step 4: Generate the usual daily output power illustrations for WT and PV utilizing weibull and beta probability distribution functions by random sampling, respectively. Furthermore, for each season, the normal probability distribution function of the usual daily load profiles should be stated. To supplement the information, the mean values and standard deviations of wind speed and solar irradiation are obtained for each hour of a typical day using the collected data, which is then used to produce discrete PDFs of wind speed and solar irradiance for each hour.

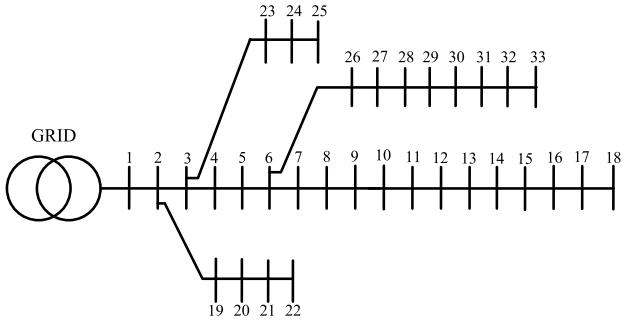

FIGURE 6. IEEE 33 bus distribution system.

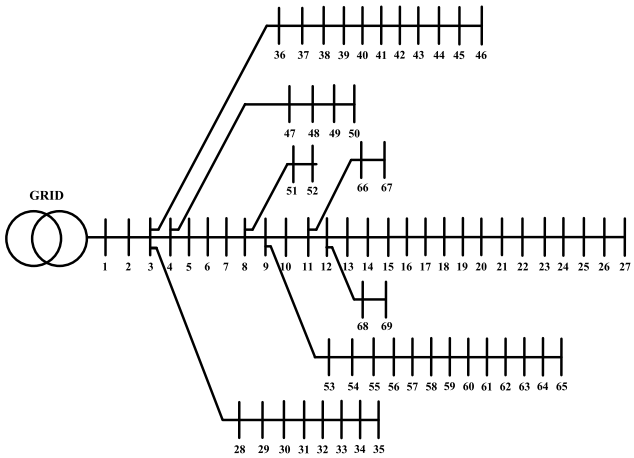

FIGURE 7. IEEE 69 bus distribution system.

TABLE 2. System parameters and initial power flow metrics of IEEE 33 and 69 bus system.

Parameters	33 bus system	69 bus system
N_B	33	69
N_{BR}	32	68
$V_{sys}(kV)$	12.66	12.66
$BaseMVA$	100	100
$P_{load}(MW)$	3.715	3.802
$Q_{load}(Mvar)$	2.30	2.695
$P_{loss}(kW)$	202.5	220.3
$V_{min,bus}(p.u.)$	0.9131	0.9105
$V_{max,bus}(p.u.)$	1	1
$V_D(p.u.)$	1.7002	1.7800
VSM_{sys}	0.6940	0.6849
$AEL_{T,noDG}(\$)$	88695	96481.4

Step 5: Specify algorithmic variables including population size and the number of iterations, and then form the initial population set. A potential solution, for example, can be represented by a vector consisting of a combination of RDG farm locations and rated power, i.e., the number of elementary RDG units at these locations.

Step 6: Compute each agent's objective function from the existing population.

Step 7: Use the AHA operators to generate new population set.

Step 8: *Steps* 6 and 7 should be repeated until the maximum number of iterations is exceeded.

Step 9: Return the best solution from the last iteration, including the optimal positions (bus locations) and rated power (RDG type and the number of elementary RDG units at each of these bus locations).

TABLE 3. Input parameters for RDG sizing and placement considering uncertainties.

Parameter	Value
$N_{iter,max}$	100
N_{pop}	50
N_{runs}	50
$Bus\ voltage\ limits\ (p.u.)$	$\pm 5\%$
$NRDGi_{max}$	10
$P_{RDGi}(kW)$	200
N_{RDGF}	2
$Total\ generation\ (MW)$	$\sum_{m=1}^{N_{DG}} S_{DG,m} \leq 3$
$v_n(m/s)$	10
$v_{ci}(m/s)$	2.7
$v_{co}(m/s)$	25
$G_{STC}(W/m^2)$	1000
$R_C(W/m^2)$	120
C_{DG} ($/kW) [30]	30
T_{DG}	10
C_E ($/kWh)	0.05
$R(\%)$	10

VI. SIMULATIONS RESULTS

IEEE 33 bus and 69 bus radial distribution systems are employed as test systems in this work. The flowchart of the algorithm is depicted in Fig. 8. The system performances are analyzed and compared to HHO-PSO and the PPSOGSA algorithms using MATLAB software to analyze the efficiency of the proposed AHA algorithm. The Newton-Raphson power flow method is adopted in this study. In addition, two types of simulations were investigated to check the validity of the proposed algorithm. Firstly, optimal RDG sizing and placement problem are simulated by considering the effect of uncertainties in RDG generation and seasonal load profiles. Secondly, under a constant power load, ideal RDG size and location are simulated without considering uncertainties. To provide a valid comparison, the initial population set size (50) and total iteration number (100) for all three algorithms are maintained constant. Furthermore, the termination condition of the algorithms is set to the maximum number of iterations.

A. RDG SIZING AND PLACEMENT CONSIDERING UNCERTAINTIES

The objective is to achieve the optimum size and location for one WT farm and one PV farm in the IEEE 33 and 69-bus system. For both WT and PV generation, P_{RDGi} is set as 200 kW with unity power factor, while $NRDGi_{max}$ is chosen as 10. This numeric values of WT units' rated power, nominal wind speed, cut-in wind speed, cut-out wind speeds, PV units solar irradiance at standard test conditions and certain irradiance point is depicted in Table 3

The wind speed and solar irradiation measurements originate from [46], which are recorded with a sample period of 5 minutes for the whole year of 2016. The year is considered to be divided into three seasons: spring (August, September, and October), summer (March, April, May, June, and July), and winter (November, December, January and February).

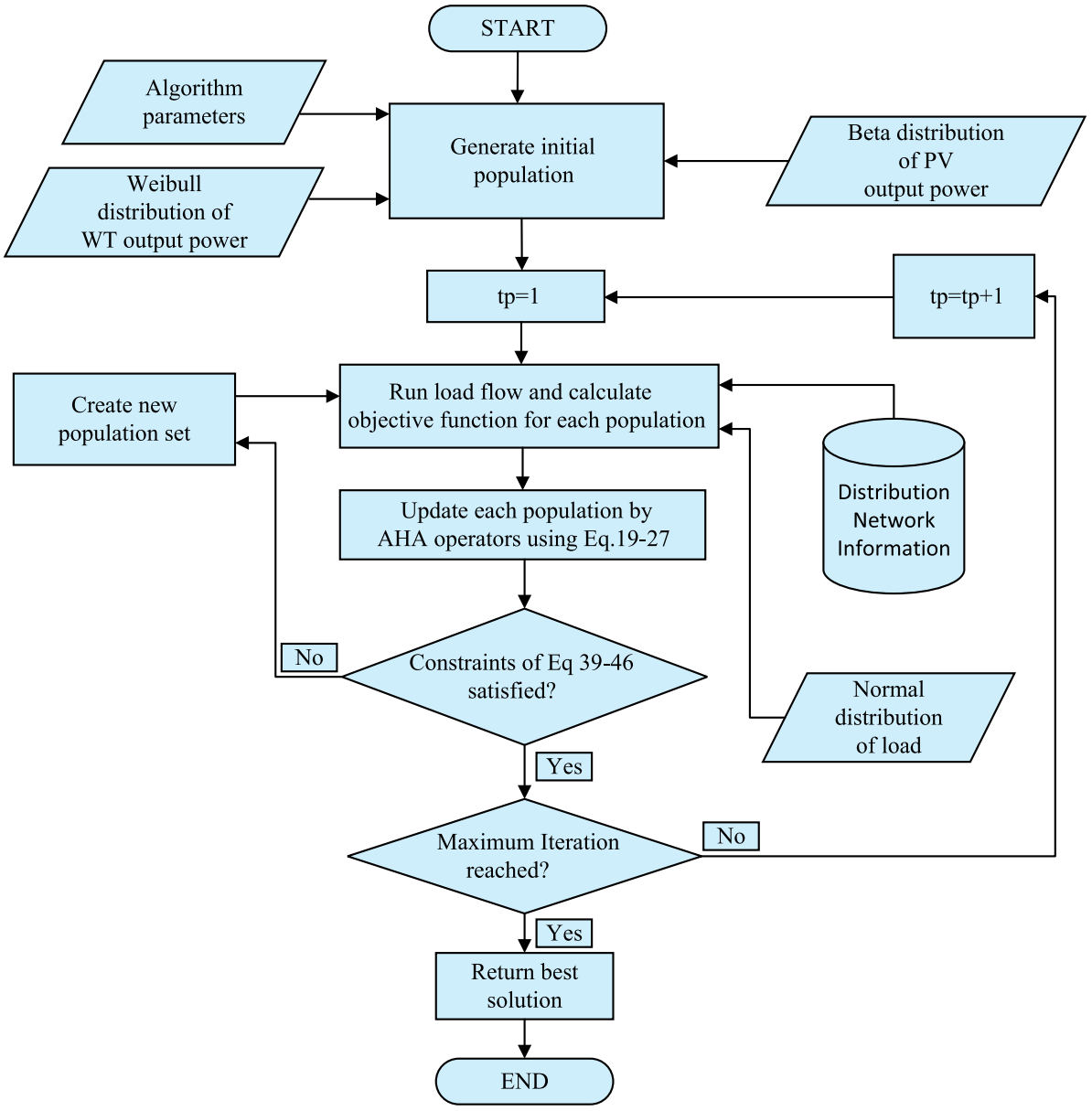

FIGURE 8. Flowchart of RDG planning optimization.

TABLE 4. IEEE 33 bus optimal size and location of RDG farms.

Algorithm	Farm	Location bus	N_{RDG}	P_{RDGF}
PPSOGSA	PV	13	5	1
	WT	29	9	1.8
HH0-PSO	PV	33	8	1.6
	WT	13	5	1
AHA	PV	11	7	1.4
	WT	6	6	1.2

TABLE 5. IEEE 33 bus optimised results of economical and technical metrics for ten years.

Index	PPSOGSA	HHO-PSO	AHA
Energy loss (MWh)	8074.1245	9539.465	**7700.4135**
Average V_D	0.096	0.14	**0.093**
Average VSM	0.921	0.912	0.932
TAES	591969.3	518682.64	**610682.342**

The mean values and standard deviations of wind speed and solar irradiation are determined for each hour of a typical day based on the collected data, which was further utilized to generate the discrete PDFs of wind speed and solar irradiance for each hour. Using typical day patterns for seasons, the projected power of WT and PV is evaluated for each year over a 10-year planning horizon. Table 4 shows the optimal size and location of RDG farms on the IEEE 33 bus using the three algorithms.

Table 5 illustrates the optimized outcomes of economic and technical metrics throughout a ten-year period. As compared to PPSOGSA and HHO-PSO, AHA yields 5.3% and 26% reduced energy losses. Furthermore, AHA outperforms

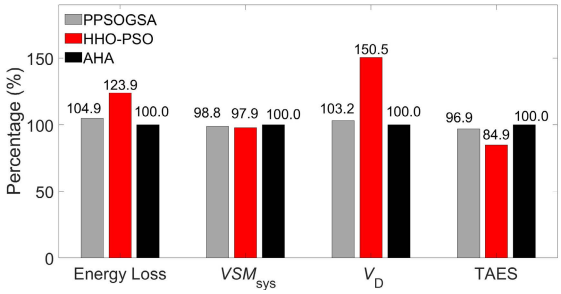

FIGURE 9. Optimal results comparison considering uncertainties for IEEE 33 bus (% differences with AHA).

TABLE 6. IEEE 69 bus optimal size and location of RDG farms.

Algorithm	Farm	Location bus	N_{RDG}	P_{RDGF}
PPSOGSA	PV	61	9	1.8
	WT	13	5	1
HH0-PSO	PV	61	9	1.8
	WT	69	6	1.2
AHA	PV	61	9	1.8
	WT	17	3	0.6

TABLE 7. IEEE 69 bus optimised results of economical and technical metrics for ten years.

Index	PPSOGSA	HHOPSO	AHA
Energy loss (MWh)	5585.996	6018.714	**5241.7885**
Average VD	0.0639	0.1125	**0.0622**
Average VSM	0.951	0.933	**0.958**
TAES	803566.442	782101.18	**821007.1**

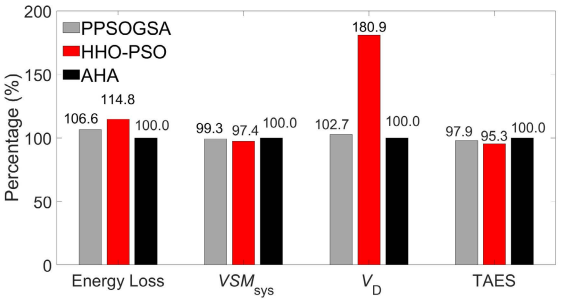

FIGURE 10. Optimal results comparison considering uncertainties for IEEE 69 bus (% differences with AHA).

PPSOGSA and HHO-PSO in terms of average voltage deviation (V_D) for each hour by 3.2% and 50.5%, respectively. In addition, as compared to the other algorithms, AHA achieved the maximum VSM_{sys} and overall energy savings value. Besides, AHA appears to require the fewest amount of elementary RDGs while still providing the optimum solution. The findings are compared with AHA results for demonstration purposes and presented in a bar diagram in Fig. 9.

Table 6 shows the optimal size and placement of RDG farms using the three methods for the IEEE 69 bus system. Table 7 presents the optimized outcomes of economic and technical metrics throughout a ten-year period. In comparison to PPSOGSA and HHO-PSO, AHA delivers 6.5% and 14.8% reduced energy losses, respectively. Besides, AHA employs the fewest number of elementary RDGs. Additionally, AHA's

TABLE 8. Input parameters for RDG sizing and placement without considering uncertainties.

Parameter	Value
$N_{iter,max}$	100
N_{pop}	50
N_{runs}	50
$Bus\ voltage\ limits\ (p.u.)$	$\pm 5\%$
$RDG\ size\ limits\ (MVA)$	$0 \leq S_{DG,max} \leq 2$
$Total\ generation\ (MVA)$	$\sum_{m=1}^{N_{DG}} S_{DG,m} \leq 3$
$RDG\ PF\ limits$	pf_{PV}=1 & $0.65 \leq pf_{WT} \leq 1$
C_{DG} ($/kW$) [30]	30
T_{DG} $(years)$	10
C_E ($/kWh$)	0.05
$R(\%)$	10

average voltage deviation (VD) for each hour is 2.7% lower and 80.8% lower than that of PPSOGSA and HHO-PSO, respectively. Furthermore, AHA outperforms all the other algorithms in terms of VSM_{sys} and overall energy savings. In a bar diagram, Fig. 8 illustrates the findings compared in percentage with respect to AHA.

B. RDG SIZING AND PLACEMENT WITHOUT CONSIDERING UNCERTAINTIES

To validate the suggested algorithm's efficiency in contrast to previous optimization techniques, the problem of RDG sizing and placement for dispatchable RDG units is investigated. Multiple PV and WT penetration levels are simulated and assessed. The PV induces solely active power, whereas the WT can accommodate both active and reactive power. Furthermore, it is anticipated that only one RDG unit can be penetrated on the same bus at a time. A potential solution set, for example, can be represented as a vector composed of three variables such as PV/WT locations, size, and the power factor of RDG units at these locations. The first variable determines the placement of RDGs on network buses. The second variable represents the power generation of RDGs at the given load level, with actual values ranging from 0 to the maximum capacity of the related RDG. Each of the third variable has a value ranging from 0 to 1 and indicates the optimal power factor of the installed WT-DG units. However, when PV-type DG units are installed, the values of that variable are always 1. Besides, it has been assumed that the load model is constant and PV's and WT's generation is not affected by natural uncertainties. The fundamental purpose of the optimization is to identify the most appropriate size and location of RDGs in order to improve the distribution system's techno-economic efficiency.

Table 8 displays the input data and cost parameters for the optimum planning problem. Two scenarios of RDG integration, including two and three PV/WTs, are investigated to demonstrate the beneficial impacts of appropriate allocation on system performance. Table 9 compares the results of the AHA simulation to other algorithms for identifying and sizing numerous RDG units in an IEEE 33 bus system. In comparison to HHO-PSO and PPSOGSA, AHA provides 15.8 KW and 3.7 KW reduced power loss

with 2 PV integration, respectively. Furthermore, when compared to HHO-PSO and PPSOGSA, AHA provides 0.8 KW and 3.3 KW reduced power loss with 3 PV integration, accordingly. Furthermore, in contrast with HHO-PSO and PPSOGSA, AHA provides 13.1 KW and 10.6 KW reduced power loss for 2 WT integration, respectively. Moreover, as compared to HHO-PSO and PPSOGSA, AHA provides 29.6 KW and 3.9 KW reduced power loss for 3 WT integration. It is significant to mention that the voltage deviation and VSM values in WT installation scenarios are substantially better due to the reactive power support. Moreover, AHA exceeds the other algorithms in terms of overall yearly energy savings value.

For IEEE 69 bus system, Table 10 compares the results of the AHA simulation to the other methods for locating and sizing several RDG units. In order to reduce power loss and voltage variation, the proposed AHA algorithm appears to outperform the rest of the algorithms studied for the 69-bus system, just as it did for the 33-bus system. In addition, AHA outperforms the other algorithms in terms of yearly energy savings and VSM value. According to the results obtained for both test systems, AHA has the lowest energy loss, lowest voltage deviation, maximum voltage stability margin, and maximum yearly energy savings, which demonstrates the algorithm's superiority over other optimization approaches.

Fig. 11 depicts the impact of RDG with optimal placements and sizes on the network voltage profile. The voltage deviation is clearly minimized with proper RDG unit connections, where the voltage magnitude on each bus is within allowed ranges of 0.95-1.05 p.u. Also, it has been identified that AHA provides the optimal solution for each case with the minimum amount of total voltage deviation. Besides, WTs provide a superior voltage profile and significantly improve the system voltage stability compared to PVs because of their ability to supply reactive power. As illustrated in Fig.12, AHA converges significantly faster than HHO-PSO and PPSOGSA for each of the systems. The findings reveal that the AHA accelerates to the near optimal solution swiftly and with consistent convergence characteristics when compared to the other two algorithms. Table 11 compares the best value, worst value and the mean value of the results along with the computational time obtained by PPSOGSA, HHO-PSO, and proposed method over 50 runs in the scenarios of 3 WT and 3 PV installation in IEEE 69 bus system. AHA appears to surpass the other two algorithms in terms of power loss value. In most circumstances, the worst AHA result is better than the best HHO-PSO and PPSOGSA results. Furthermore, AHA outperforms HHO-PSO and PPSOGSA in terms of elapsed time, with HHO-PSO having the longest computing time of all the methods. These statistical indicators strongly suggest that the proposed method outperforms PPSOGSA and HHO-PSO in terms of providing better and more consistent results.

The tested results are obtained using various scenarios in order to demonstrate the algorithm's effectiveness. The suggested technique, known as the Artificial Hummingbird Algorithm, has been found to be more beneficial than previous algorithms for RDG sizing and placement, regardless of whether weather or load uncertainty is included. For added information, the test is completed by considering DGs as dispatchable units (2PV, 3 PV, 2WT, 3 WT) for both the IEEE 33 and IEEE 69 bus systems. Furthermore, AHA gives superior solutions and enhances the techno-economic aspects of distribution networks in all the scenarios evaluated.

TABLE 9. IEEE 33 bus optimal results for RDG placement without uncertainties.

Case	Algorithm	Optimal result			Loss (kW)	Deviation	VSM	TAES
		Bus	Size (MVA)	p.f.				
2 PV	HHO PSO	32	1.5273,	1	135.3	0.2863	0.9355	29420.13
		18	1.2363	1				
	PSO PGA	32	1.6524	1	123.2	0.1808	0.9396	34724.09
		13	1.3476	1				
	AHA	13	1.3421	1	**119.5**	**0.174**	**0.9398**	**36338.3**
		31	1.6577	1				
3 PV	HHO PSO	32		1	111.9	0.2601	0.9351	39691
		13	0.2417	1				
		33	1.25211.2323	1				
	PSO PGA	15	1.65234	1	114.4	0.1896	0.9414	38600.06
		31	1.5644	1				
		28	0.4132	1				
	AHA	10	0.8607	1	**111.1**	**0.1594**	**0.9393**	**40010.3**
		32	1.5285	1				
		16	0.609	1				
2 WT	HHO PSO	12	0.8873	0.7352	63.9	0.2715	0.9462	60860.957
		33	1.9953	0.8791				
	PSO PGA	30	1.5849	0.9671	53.3	0.1344	0.945	64677.555
		11	1.361	0.9499				
	AHA	29	1.7785	0.9315	**46.8**	**0.1312**	**0.947**	**68378.5**
		12	1.1715	0.9403				
3 WT	HHO PSO	11	1.8961	0.95	59.7	0.2679	0.9393	62530
		19	0.2196	0.6516				
		32	0.8653	0.9284				
	PSO PGA	29	1.8383	0.8497	35.4	01548	0.9253	73200
		6	0.1166	0.9767				
		12	0.9686	0.9123				
	AHA	8	0.9836	0.9094	**30.3**	**0.0993**	**0.9171**	**75426.2**
		29	1.5377	0.8843				
		16	0.4739	0.8625				

TABLE 10. IEEE 69 bus optimal results for RDG placement without uncertainties.

Case	Algorithm	Optimal result			Loss (kW)	Deviation	VSM	TAES
		Bus	Size (MVA)	p.f.				
2 PV	HHO PSO	65	1.7056	1	108.7	0.2604	0.977	48872.69
		13	1.2327	1				
	PSO PGA	65	1.69	1	110.1	0.2391	0.977	48255.15
		13	1.31	1				
	AHA	14	0.9827	1	**95.1**	**0.177**	**0.977**	**54845.48**
		64	1.9862	1				
3 PV	HHO PSO	68	1.0746	1	103.6	0.2999	0.977	51111.28
		27	0.3007	1				
		65	1.6229	1				
	PSO PGA	65	1.0443	1	92.7	0.1528	0.9733	55887.59
		60	1.3383	1				
		23	0.6172	1				
	AHA	19	0.6833	1	**91.2**	**0.1307**	**0.9758**	**60934.07**
		64	0.4941	1				
		61	1.792	1				
2 WT	HHO PSO	64	1.8665	0.9809	59.6	0.3317	0.9771	70370.8863
		20	0.9951	0.9756				
	PSO PGA	15	0.7282	0.8687	23.7	0.152	0.9722	86089.27
		64	1.9971	0.784				
	AHA	14	0.9937	0.6746	**18.7**	**0.0906**	**0.9772**	**88298.91**
		63	1.9984	0.8991				
3 WT	HHO PSO	46	0.3136	0.9201	70.7	0.2679	0.959	65527.04
		65	1.3817	0.9746				
		27	0.8725	0.8119				
	PSO PGA	65	1.9565	0.8611	47.1	0.2106	0.9722	75841.93
		45	0.1405	0.8699				
		22	0.7262	0.8373				
	AHA	18	0.6726	0.7213	**11.8**	**0.0899**	**0.9772**	**91328.73**
		63	1.4962	0.7827				
		58	0.8242	0.7936				

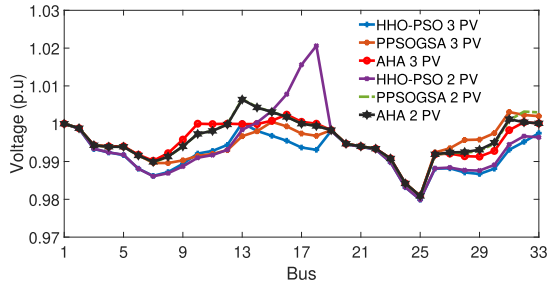

(a) IEEE 33 bus PV unit installation

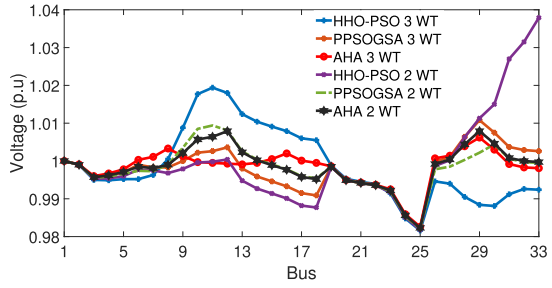

(b) IEEE 33 bus WT unit installation

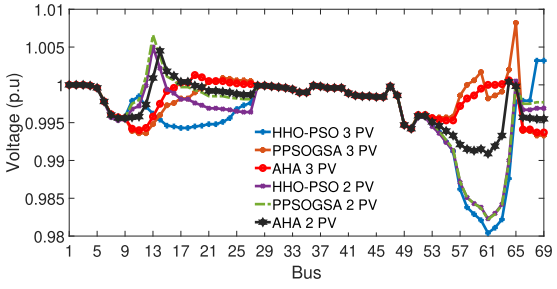

(c) IEEE 69 bus PV unit installation

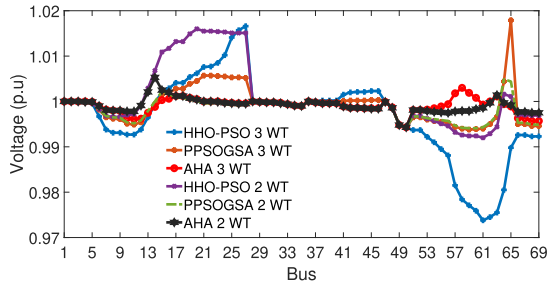

(d) IEEE 69 bus WT unit installation

FIGURE 11. Voltage profile.

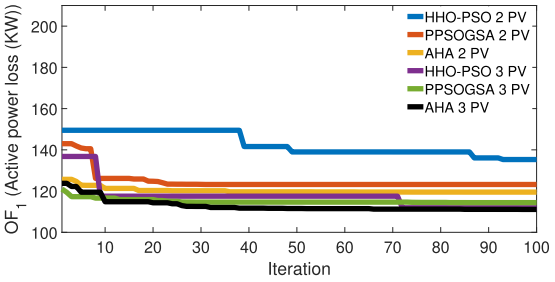

(a) IEEE 33 bus PV unit installation

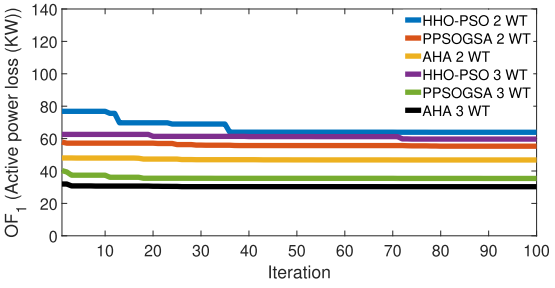

(b) IEEE 33 bus WT unit installation

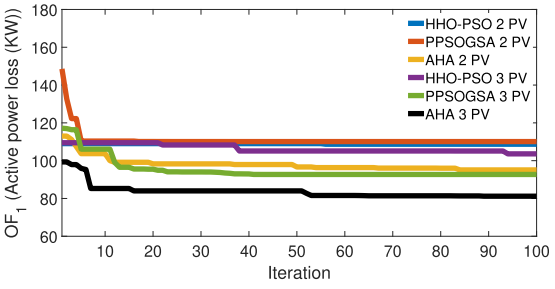

(c) IEEE 69 bus PV unit installation

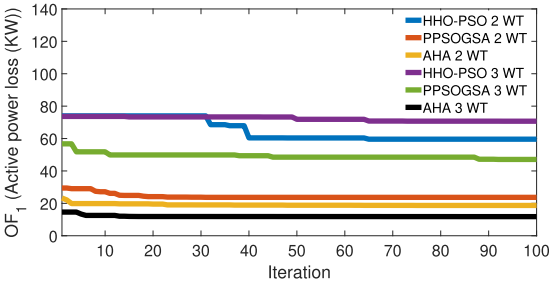

(d) IEEE 69 bus WT unit installation

FIGURE 12. Convergence curve.

TABLE 11. Statistics of PPSOGSA, HHO-PSO and AHA.

Case	Method	Best (kW)	Worst (kW)	Mean (kW)	Mean elapsed time (s)
3 WT	HHO-PSO	70.7	76.4	72.6	10.8
	PPSOGSA	47.1	54.2	51.4	9.7
	AHA	**11.8**	**16.4**	**12.8**	**7.8**
3 PV	HHO-PSO	103.6	109.6	104.7	7.4
	PPSOGSA	92.7	101.6	94.8	7.1
	AHA	**91.2**	**93.4**	**92.1**	**5.7**

C. ALGORITHM PARAMETERS VARIATION

The robustness of the AHA algorithm parameters is verified by varying the probability ($0 \sim 1$) values of the flight and foraging techniques. Fig. 13 depicts how the algorithmic parameters affect the power loss values of 3 PV and 3 WT RDG allocation and sizing in a 69 bus test system. The guided foraging technique probability and the diagonal flight probability were adjusted in this analysis to detect the variance in the results. The findings reveal that modifying the algorithmic parameters has little effect on the OF_1 values. According to the findings, the OF_1 results had an average standard deviation of 0.247 and 0.513 for 3 WT and 3 PV installments, respectively. Besides, during the simulation, it was also observed that changing the algorithmic parameters slows down the optimization process. As a consequence, it is possible to infer that the algorithmic settings should be kept as default in order to achieve the best results.

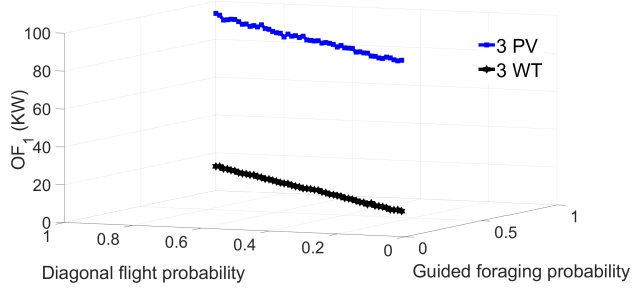

FIGURE 13. AHA algorithmic parameters & OF_1.

VII. CONCLUSION

This paper proposes a novel method for determining the appropriate size and location of RDGs in distribution networks. Four criteria were used to determine the optimal DG size and placement: minimization of voltage deviation, minimization of total active power loss, maximization of voltage stability margin value and maximization of total annual energy savings. The results of the proposed AHA algorithm were compared to those of two recent algorithms, HHO-PSO and PPSOGSA. Two simulation types were considered: with uncertainties and without uncertainties. According to the findings obtained, AHO outperforms all the algorithms for all the objectives with early convergence characteristics for both the simulation types. Therefore, the suggested technique may be recommended for optimal location and sizing of RDGs in real distribution systems considering both weather and load uncertainties.

The implications of concurrent installation of PV and WT on existing distribution networks may be studied in the future using real-time load and weather data. Besides, the weighted factors of the techno-economic indices of the objective function can be modified to assess the results variation of the suggested techniques. Moreover, future works may include energy storage technologies for distribution systems.

ACKNOWLEDGMENT

The authors state that they have no known competing financial interests or personal relationships that could have influenced the work presented in this study.

REFERENCES

[1] V. K. Mehta and R. Mehta, *Principles of Power System: Including Generation, Transmission, Distribution, Switchgear and Protection: For BE/B. Tech., AMIE and Other Engineering Examinations*. Chennai, India: S. Chand Publishing, 2005.

[2] J. P. Lopes, N. Hatziargyriou, J. Mutale, P. Djapic, and N. Jenkins, "Integrating distributed generation into electric power systems: A review of drivers, challenges and opportunities," *Electr. Power Syst. Res.*, vol. 77, no. 9, pp. 1189–1203, 2007.

[3] O. Ellabban, H. Abu-Rub, and F. Blaabjerg, "Renewable energy resources: Current status, future prospects and their enabling technology," *Renew. Sustain. Energy Rev.*, vol. 39, pp. 748–764, Nov. 2014.

[4] S. Weitemeyer, D. Kleinhans, T. Vogt, and C. Agert, "Integration of renewable energy sources in future power systems: The role of storage," *Renew. Energy*, vol. 75, pp. 14–20, Mar. 2015.

[5] M. Liserre, T. Sauter, and J. Y. Hung, "Future energy systems: Integrating renewable energy sources into the smart power grid through industrial electronics," *IEEE Ind. Electron. Mag.*, vol. 4, no. 1, pp. 18–37, Mar. 2010.

[6] A. Šare, G. Krajačić, T. Pukšec, and N. Duić, "The integration of renewable energy sources and electric vehicles into the power system of the dubrovnik region," *Energy, Sustainability Soc.*, vol. 5, no. 1, pp. 1–16, Dec. 2015.

[7] J. Dudiak and M. Kolcun, "Integration of renewable energy sources to the power system," in *Proc. 14th Int. Conf. Environ. Electr. Eng.*, May 2014, pp. 148–151.

[8] P. Paliwal, N. P. Patidar, and R. K. Nema, "Planning of grid integrated distributed generators: A review of technology, objectives and techniques," *Renew. Sustain. Energy Rev.*, vol. 40, pp. 557–570, Dec. 2014.

[9] N. Mararakanye and B. Bekker, "Renewable energy integration impacts within the context of generator type, penetration level and grid characteristics," *Renew. Sustain. Energy Rev.*, vol. 108, pp. 441–451, Jul. 2019.

[10] G. Allan, I. Eromenko, M. Gilmartin, I. Kockar, and P. McGregor, "The economics of distributed energy generation: A literature review," *Renew. Sustain. Energy Rev.*, vol. 42, pp. 543–556, Feb. 2015.

[11] M. F. Akorede, H. Hizam, and E. Pouresmaeil, "Distributed energy resources and benefits to the environment," *Renew. Sustain. Energy Rev.*, vol. 14, no. 2, pp. 724–734, Feb. 2010.

[12] R. H. A. Zubo, G. Mokryani, H.-S. Rajamani, J. Aghaei, T. Niknam, and P. Pillai, "Operation and planning of distribution networks with integration of renewable distributed generators considering uncertainties: A review," *Renew. Sustain. Energy Rev.*, vol. 72, pp. 1177–1198, May 2017.

[13] S. Esmaeili, A. Anvari-Moghaddam, and S. Jadid, "Optimal operational scheduling of reconfigurable multi-microgrids considering energy storage systems," *Energies*, vol. 12, no. 9, p. 1766, May 2019.

[14] J. Najafi, A. Peiravi, A. Anvari-Moghaddam, and J. M. Guerrero, "Resilience improvement planning of power-water distribution systems with multiple microgrids against hurricanes using clean strategies," *J. Cleaner Prod.*, vol. 223, pp. 109–126, Jun. 2019.

[15] A. S. Hassan, E. A. Othman, F. M. Bendary, and M. A. Ebrahim, "Optimal integration of distributed generation resources in active distribution networks for techno-economic benefits," *Energy Rep.*, vol. 6, pp. 3462–3471, Nov. 2020.

[16] A. R. Jordehi, "How to deal with uncertainties in electric power systems? A review," *Renew. Sustain. Energy Rev.*, vol. 96, pp. 145–155, Nov. 2018.

[17] A. Soroudi, M. Aien, and M. Ehsan, "A probabilistic modeling of photo voltaic modules and wind power generation impact on distribution networks," *IEEE Syst. J.*, vol. 6, no. 2, pp. 254–259, Jun. 2012.

[18] A. Maleki, M. G. Khajeh, and M. Ameri, "Optimal sizing of a grid independent hybrid renewable energy system incorporating resource uncertainty, and load uncertainty," *Int. J. Electr. Power Energy Syst.*, vol. 83, pp. 514–524, Dec. 2016.

[19] M. R. Elkadeem, M. Abd Elaziz, Z. Ullah, S. Wang, and S. W. Sharshir, "Optimal planning of renewable energy-integrated distribution system considering uncertainties," *IEEE Access*, vol. 7, pp. 164887–164907, 2019.

[20] J. Radosavljevic, N. Arsic, M. Milovanovic, and A. Ktena, "Optimal placement and sizing of renewable distributed generation using hybrid Metaheuristic algorithm," *J. Modern Power Syst. Clean Energy*, vol. 8, no. 3, pp. 499–510, 2020.

[21] E. S. Ali, S. M. A. Elazim, and A. Y. Abdelaziz, "Optimal allocation and sizing of renewable distributed generation using ant lion optimization algorithm," *Electr. Eng.*, vol. 100, no. 1, pp. 99–109, Mar. 2018.

[22] A. El-Fergany, "Optimal allocation of multi-type distributed generators using backtracking search optimization algorithm," *Int. J. Electr. Power Energy Syst.*, vol. 64, pp. 1197–1205, Jan. 2015.

[23] F. S. Abu-Mouti and M. E. El-Hawary, "Modified artificial bee colony algorithm for optimal distributed generation sizing and allocation in distribution systems," in *Proc. IEEE Electr. Power Energy Conf. (EPEC)*, Oct. 2009, pp. 1–9.

[24] R. Sanjay, T. Jayabarathi, T. Raghunathan, V. Ramesh, and N. Mithulananthan, "Optimal allocation of distributed generation using hybrid grey wolf optimizer," *IEEE Access*, vol. 5, pp. 14807–14818, 2017.

[25] M. Imran A and M. Kowsalya, "Optimal size and siting of multiple distributed generators in distribution system using bacterial foraging optimization," *Swarm Evol. Comput.*, vol. 15, pp. 58–65, Apr. 2014.

[26] D. R. Prabha, T. Jayabarathi, R. Umamageswari, and S. Saranya, "Optimal location and sizing of distributed generation unit using intelligent water drop algorithm," *Sustain. Energy Technol. Assessments*, vol. 11, pp. 106–113, Sep. 2015.

[27] S. A. ChithraDevi, L. Lakshminarasimman, and R. Balamurugan, "Stud krill herd algorithm for multiple DG placement and sizing in a radial distribution system," *Eng. Sci. Technol., Int. J.*, vol. 20, no. 2, pp. 748–759, Apr. 2017.

[28] M. H. Moradi and M. Abedini, "A combination of genetic algorithm and particle swarm optimization for optimal distributed generation location and sizing in distribution systems with fuzzy optimal theory," *Int. J. Green Energy*, vol. 9, no. 7, pp. 641–660, Oct. 2012.
[29] S. Kaur, G. Kumbhar, and J. Sharma, "A MINLP technique for optimal placement of multiple DG units in distribution systems," *Int. J. Electr. Power Energy Syst.*, vol. 63, pp. 609–617, Dec. 2014.
[30] S. Kumar, K. K. Mandal, and N. Chakraborty, "Optimal DG placement by multi-objective opposition based chaotic differential evolution for techno-economic analysis," *Appl. Soft Comput.*, vol. 78, pp. 70–83, May 2019.
[31] D. K. Khatod, V. Pant, and J. Sharma, "Evolutionary programming based optimal placement of renewable distributed generators," *IEEE Trans. Power Syst.*, vol. 28, no. 2, pp. 683–695, May 2013.
[32] A. Y. Abdelaziz, Y. G. Hegazy, W. El-Khattam, and M. M. Othman, "Optimal allocation of stochastically dependent renewable energy based distributed generators in unbalanced distribution networks," *Electr. Power Syst. Res.*, vol. 119, pp. 34–44, Feb. 2015.
[33] P. Kayal and C. K. Chanda, "Optimal mix of solar and wind distributed generations considering performance improvement of electrical distribution network," *Renew. Energy*, vol. 75, pp. 173–186, Mar. 2015.
[34] A. Ali, K. Mahmoud, and M. Lehtonen, "Optimal planning of inverter-based renewable energy sources towards autonomous microgrids accommodating electric vehicle charging stations," *IET Gener., Transmiss. Distrib.*, vol. 16, no. 2, pp. 219–232, Jan. 2022.
[35] A. Ali, K. Mahmoud, and M. Lehtonen, "Optimization of photovoltaic and wind generation systems for autonomous microgrids with PEV-parking lots," *IEEE Syst. J.*, early access, Aug. 13, 2021, doi: 10.1109/JSYST.2021.3097256.
[36] S. R. Biswal, G. Shankar, R. M. Elavarasan, and L. Mihet-Popa, "Optimal allocation/sizing of DGs/capacitors in reconfigured radial distribution system using quasi-reflected slime mould algorithm," *IEEE Access*, vol. 9, pp. 125658–125677, 2021.
[37] M. Zellagui, N. Belbachir, and C. Ziad El-Bayeh, "Optimal allocation of RDG in distribution system considering the seasonal uncertainties of load demand and solar-wind generation systems," in *Proc. IEEE EUROCON 19th Int. Conf. Smart Technol.*, Jul. 2021, pp. 471–477.
[38] A. A. Lekvan, R. Habibifar, M. Moradi, M. Khoshjahan, S. Nojavan, and K. Jermsittiparsert, "Robust optimization of renewable-based multi-energy micro-grid integrated with flexible energy conversion and storage devices," *Sustain. Cities Soc.*, vol. 64, Jan. 2021, Art. no. 102532.
[39] S. Galvani, A. Bagheri, M. Farhadi-Kangarlu, and N. Nikdel, "A multi-objective probabilistic approach for smart voltage control in wind-energy integrated networks considering correlated parameters," *Sustain. Cities Soc.*, vol. 78, Mar. 2022, Art. no. 103651.
[40] J. Geng, T. Zheng, J. Cao, Y. Yang, Y. Jin, and J. Fu, "Research on multi-objective operation optimization of multi energy integrated service stations based on autonomous collaborative control," *Energy Rep.*, vol. 8, pp. 278–284, Aug. 2022.
[41] P. Dinakara, "Optimal renewable resources placement in distribution networks by combined power loss index and whale optimization algorithms," *J. Electr. Syst. Inf. Technol.*, vol. 5, no. 2, pp. 175–191, Sep. 2018.
[42] M. Tolba, H. Rezk, V. Tulsky, A. Diab, A. Abdelaziz, and A. Vanin, "Impact of optimum allocation of renewable distributed generations on distribution networks based on different optimization algorithms," *Energies*, vol. 11, no. 1, p. 245, Jan. 2018.
[43] S. Nawaz, D. A. K. Bansal, and D. M. P. Sharma, "A novel approach for multiple DG allocation in real distribution system," *Int. J. Eng. Technol.*, vol. 9, no. 2, pp. 963–968, Apr. 2017.
[44] A. El-Fergany, "Multi-objective allocation of multi-type distributed generators along distribution networks using backtracking search algorithm and fuzzy expert rules," *Electric Power Compon. Syst.*, vol. 44, no. 3, pp. 252–267, Feb. 2016.
[45] P. P. Biswas, P. N. Suganthan, R. Mallipeddi, and G. A. J. Amaratunga, "Optimal reactive power dispatch with uncertainties in load demand and renewable energy sources adopting scenario-based approach," *Appl. Soft Comput.*, vol. 75, pp. 616–632, Feb. 2019.
[46] Open Data Sets. *IEEE PES Intelligent Systems Subcommittee*. Accessed: Feb. 3, 2022. [Online]. Available: https://site.ieee.org/pes-iss/data-sets/
[47] Y. M. Atwa, E. F. El-Saadany, M. M. A. Salama, and R. Seethapathy, "Optimal renewable resources mix for distribution system energy loss minimization," *IEEE Trans. Power Syst.*, vol. 25, no. 1, pp. 360–370, Feb. 2010.
[48] Power Systems Test Case Archive. *Reliability Test System*. Accessed: Feb. 3, 2022. [Online]. Available: http://labs.ece.uw.edu/pstca/rts/pg_tcarts.htm
[49] W. Zhao, L. Wang, and S. Mirjalili, "Artificial hummingbird algorithm: A new bio-inspired optimizer with its engineering applications," *Comput. Methods Appl. Mech. Eng.*, vol. 388, Jan. 2022, Art. no. 114194.
[50] H. M. Ayres, W. Freitas, M. C. D. Almeida, and L. C. P. D. Silva, "Method for determining the maximum allowable penetration level of distributed generation without steady-state voltage violations," *IET Gener., Transmiss. Distrib.*, vol. 4, no. 4, p. 495, 2010.
[51] M. H. Hauqe, "A linear static voltage stability margin for radial distribution systems," in *Proc. IEEE Power Eng. Soc. Gen. Meeting*, Jun. 2006, p. 6.
[52] V. Vita, "Development of a decision-making algorithm for the optimum size and placement of distributed generation units in distribution networks," *Energies*, vol. 10, no. 9, p. 1433, 2017.
[53] K. Narayanan, S. A. Siddiqui, and M. Fozdar, "Hybrid islanding detection method and priority-based load shedding for distribution networks in the presence of DG units," *IET Gener., Transmiss. Distrib.*, vol. 11, no. 3, pp. 586–595, Feb. 2017.

MD. SHADMAN ABID (Student Member, IEEE) is currently pursuing the B.Sc. degree in electrical and electronic engineering (EEE) with the Islamic University of Technology (IUT), Gazipur, Bangladesh. His main research interests include power system optimization, power quality, artificial intelligence, electric vehicles, distributed generation, power system distribution automation, and microgrids.

HASAN JAMIL APON is currently pursuing the B.Sc. degree in electrical and electronic engineering (EEE) with the Islamic University of Technology (IUT), Gazipur, Bangladesh. His main research interests include power system optimization, power quality, electric vehicles, distributed generation, and microgrids.

KHANDAKER ADIL MORSHED is currently pursuing the B.Sc. degree in electrical and electronic engineering (EEE) with the Islamic University of Technology (IUT), Gazipur, Bangladesh. His main research interests include power system optimization, power quality, electric vehicles, distributed generation, and microgrids.

ASHIK AHMED received the M.Sc. degree in electrical and electronic engineering from the King Fahd University of Petroleum and Minerals, Dharhan, Saudi Arabia, in 2010, and the Ph.D. degree in electrical and electronic engineering from the Islamic University of Technology (IUT), Gazipur, Bangladesh, in 2016. He is currently a Professor with the Department of Electrical and Electronic Engineering, IUT. His research interests include engineering optimization, artificial neural networks, power system stability and control, FACTS devices, and non-linear control.